



Effects of magnetism and doping on the electron-phonon coupling in BaFe₂As₂

L. Boeri,¹ M. Calandra,² I. I. Mazin,³ O. V. Dolgov,¹ and F. Mauri²

¹Max-Planck-Institut für Festkörperforschung, Heisenbergstraße 1, D-70569 Stuttgart, Germany

²CNRS, Institut de Minéralogie et de Physique des Milieux Condensés, case 115, 4 place Jussieu, 75252 Paris Cedex 05, France

³Naval Research Laboratory, 4555 Overlook Avenue SW, Washington, DC 20375, USA

(Received 12 April 2010; revised manuscript received 4 June 2010; published 14 July 2010)

We calculate the effect of local magnetic moments on the electron-phonon coupling in doped BaFe₂As₂ using the density-functional perturbation theory. We show that the magnetism enhances the total electron-phonon coupling by $\sim 50\%$, up to $\lambda \lesssim 0.35$, still not enough to explain the high critical temperature, but strong enough to have a non-negligible effect on superconductivity, for instance, by frustrating the coupling with spin fluctuations and inducing order-parameter nodes. The enhancement comes not from the phonon softening but mostly from a renormalization of the electron-phonon matrix elements. We also investigate, in the rigid band approximation, the effect of doping, and find that λ versus doping does not mirror the behavior of the density of states; while the latter decreases upon electron doping, the former does not, and even increases slightly.

DOI: [10.1103/PhysRevB.82.020506](https://doi.org/10.1103/PhysRevB.82.020506)

PACS number(s): 74.70.Xa, 63.20.kd, 63.20.dk, 74.20.Pq

The simultaneous presence of high- T_c superconductivity and magnetism in the phase diagram of the Fe-based superconductors suggests that magnetism plays an important role in determining the superconducting properties. Phonons have been excluded early on as possible mediators, on the basis of first-principles nonmagnetic (NM) calculations for the undoped compound,^{1,2} but the experimental situation is still far from settled in this regard.^{3–5}

Density-functional theory (DFT) calculations correctly reproduce several properties of Fe pnictides, such as the magnetic pattern in the parent compounds and the geometry of the Fermi surface. The interplay of magnetic and elastic properties is however puzzling:⁶ on one hand, experiments measure weak magnetic moments ($m \sim 0.3\text{--}1.0 \mu_B$) in the spin-density wave (SDW) state and no long-range magnetic order in the superconducting samples, while spin-polarized local spin density approximation (LSDA) calculations predict large magnetic moments at all dopings ($m \sim 2.0 \mu_B$). On the other hand, the same spin-polarized LSDA calculations predict equilibrium structures and phonon densities of states that are much closer to the experiment than those predicted by nonmagnetic calculations.^{7–9} A possible way to reconcile these two apparently conflicting results is an itinerant picture, in which the Fe atoms nevertheless have large local magnetic moments that order below the Neel temperature in the undoped compound, but survive locally at all dopings.^{10,11} But this point of view immediately raises the question of whether the estimate of electron-phonon (e-ph) matrix elements given by early nonmagnetic [rather than paramagnetic (PM), i.e., with the local Fe moment entirely suppressed] DFT calculations is representative of the actual compounds because the spin part of the crystal potential is much more sensitive to the ionic displacements than the charge part. It has been argued that such magnetoelastic (spin-phonon) effects may seriously enhance coupling with electrons and play a substantial role in superconductivity.^{12,13}

In this Rapid Communication, we calculate from first principles the e-ph coupling constant in antiferromagnetic (AFM) and NM BaFe₂As₂, using the linear-response method.¹⁴ We confirm that magnetism strongly affects the

phonon frequencies, leading to a renormalization of the modes that involve Fe-As vibrations,^{7–9} but we also find a strong effect on the e-ph matrix elements (apart from the indirect effect of the phonon softening), leading to a $\sim 50\%$ increase with respect to the NM values. Using a rigid-band model, we show that the e-ph coupling constant λ as a function of doping does not follow the density of states. Finally, we estimate the e-ph coupling in the PM state by combining the *nonmagnetic* band structure (eigenenergies and eigenfunctions) with the *magnetic* phonon spectra and self-consistent potentials. For the relevant values of doping, we estimate an upper bound to the e-ph coupling constant $\lambda = 0.35$, i.e., not high enough to explain superconductivity, but not sufficiently weak to be neglected. For instance, e-ph interaction may be one of the factors responsible for experimentally observed gap anisotropy.

In order to disentangle the structural and magnetic effects, we used the high-temperature tetragonal structure^{15,16} in all our calculations. In order to estimate the effect of the SDW ordering vector on the e-ph properties, along with the NM calculations, we have considered two different AFM patterns: the checkerboard one (AFMc), in which the nearest-neighbor Fe spins are antiparallel, and the experimentally observed one (AFM stripe, AFMs), in which spins are aligned (anti)ferromagnetically along the (y)x edge of the square Fe planes. The stabilization energies with respect to the NM solutions are 90 meV/Fe atom and 130 meV/Fe atom, respectively.

All calculations were performed in the generalized gradient approximation¹⁷ using plane-waves¹⁸ and ultrasoft pseudopotentials.¹⁹ We employed a cutoff of 40 (480) Ry for the wave functions (charge densities). The electronic integration was performed over an 8^3 \mathbf{k} mesh with a 0.01 Ry Hermitian-Gaussian smearing in the NM and AFMc cases while for the AFMs case we used a $8 \times 4 \times 8$ \mathbf{k} mesh with a 0.01 Ry Hermitian-Gaussian smearing. Finer grids (20^3 and $20 \times 10 \times 20$) were used for evaluating the densities of states (DOSs) and the phonon linewidths. Dynamical matrices and e-ph linewidths were calculated on 4^3 (NM and AFMc cases) and 2^3 (AFMs case) uniform grids in \mathbf{q} space. Phonon fre-

TABLE I. Calculated properties of BaFe₂As₂. m is the integral over the cell of the absolute value of the magnetization, $N_{\sigma}(0)$ is the DOS in states/(spin eV Fe atom), λ is the electron-phonon coupling, and ω_m is the logarithmic-averaged phonon frequency. In addition to the three fully self-consistent calculations we report here three model calculations (see text): PM1 utilizes the wave functions, one-electron energies and phonon frequencies from the NM calculations, and the deformation potentials from the AFMc calculations. PM2 and PM3 use one-electron energies and wave functions from the NM calculations, and phonon frequencies and deformation potentials from the AFMc and AFMs calculations, respectively.

Magnetic order	m (μ_B)	$N_{\sigma}(0)$ (eV^{-1})	λ	ω_m (K)	$\lambda/N_{\sigma}(0)$
NM	0.0	1.18	0.18	194	0.15
AFMc	2.4	1.36	0.33	179	0.24
AFMs	2.6	0.68	0.18	180	0.26
PM1		1.18	0.27	206	0.23
PM2		1.18	0.27	195	0.23
PM3		1.18	0.31	170	0.26

quencies throughout the Brillouin zone were obtained by Fourier interpolation. The (perturbed) potentials and charge densities, as well as the phonon frequencies, were calculated self-consistently at zero doping ($\delta=0$); the effect of doping on the e-ph coupling was then estimated using the rigid-band approximation.

The band structures at $\delta=0$ (not shown) agree with previous calculations.^{11,20} The corresponding magnetic moments and DOSs at the Fermi level are reported in Table I.²¹ The phonon dispersion for NM, AFMc, and AFMs cases are shown in the left panels of Fig. 1; the remaining panels show the (partial) densities of states and Eliashberg functions. Our results agree with previous calculations in the same crystallographic structures (adding orthorhombicity additionally changes phonon dispersions, see Refs. 8 and 9). Magnetism has the biggest effect on phonon modes that involve Fe-As vibrations; there is a pronounced softening of a branch originally located at ~ 25 meV along the Γ -Z line in the NM calculation, down to ~ 20 meV in both AFMc and AFMs calculations. This branch corresponds to out-of-plane vibrations of the As atoms. The in-plane Fe-As modes at low and high energy are sensitive not only to the size, but also to the pattern, of the magnetic moment. Indeed, when the order is AFMs, Fe vibrations along the AFM direction harden, whereas those along the FM direction soften, while for the As vibrations it is the opposite.

The shift of phonon frequencies in the AFM calculations has often been considered an indication of an enhanced e-ph coupling in the magnetic phase^{12,25} but no explicit calculations of the e-ph coupling constant in the magnetic case have been reported so far. In this work, we have calculated from first principles the same-spin component of the Eliashberg spectral function,

$$\alpha^2 F_{\sigma\sigma}(\omega) = \frac{1}{N_{\sigma}(0)N_{k,k+q,\nu}} \sum_{k,n} |g_{kn,k+q,\nu}^{\nu,\sigma}|^2 \times \delta(\varepsilon_{kn}^{\sigma}) \delta(\varepsilon_{k+q,m}^{\sigma}) \delta(\omega - \omega_{q\nu}),$$

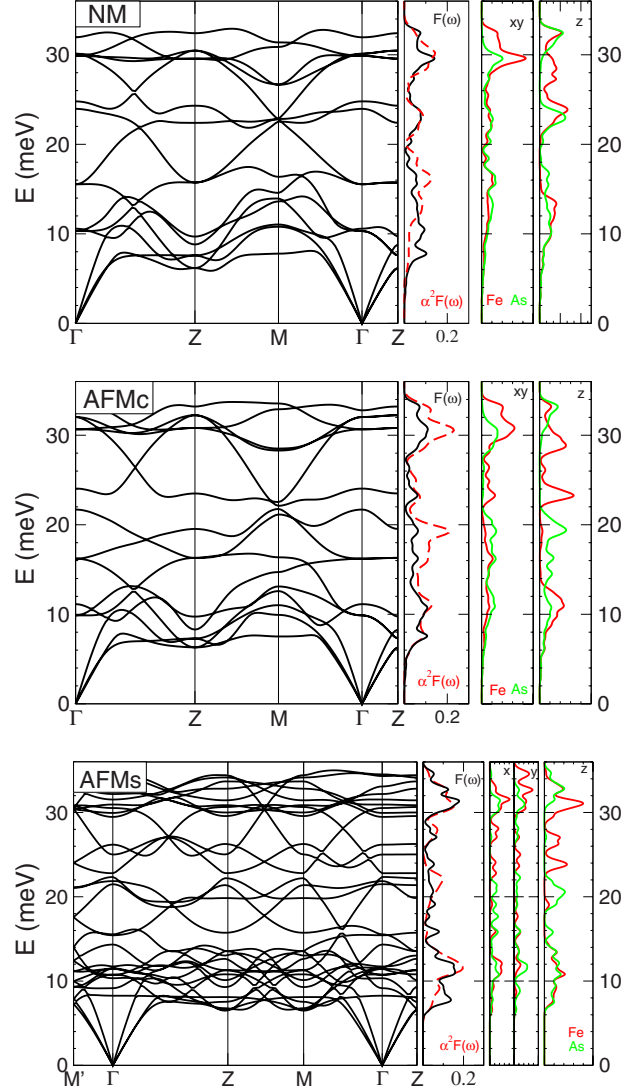


FIG. 1. (Color online) Phonon properties of undoped BaFe₂As₂ for different magnetic patterns: NM, AFMc, and AFMs. From left to right: the phonon dispersions; the total phonon densities of states, $F(\omega)$ (red, dashed) and Eliashberg function, $\alpha^2 F(\omega)$ (black, solid); partial contributions of Fe (red, dark) and As (green, light) ions to the total $F(\omega)$ projected onto Cartesian axes (the Ba contribution is limited to $\omega \leq 10$ meV and not affected by magnetic order). The dispersions are shown in the same Brillouin zone for the three patterns. The k points are selected so that they are physically the same in all three structures; the magnetic structure makes the two Γ -M directions inequivalent in the AFMs; the spins are aligned AFM (FM) in the x (y) direction. In this coordinate system, the points are: $\Gamma=(0,0,0)$; $Z=(0,0,\pi/c)$ or $(\pi/a,\pi/a,0)$; $M=(\pi/a,0,0)$; $M'=(0,\pi/2a,0)$, where a is the length of the shortest Fe-Fe bond and c is the Fe-Fe interlayer distance.

$$g_{kn,k+q,m}^{\nu,\sigma} = \langle \mathbf{k}^{\sigma n} | \delta V_{\sigma} / \delta e_{q\nu} | \mathbf{k} + \mathbf{q}^{\sigma m} \rangle / \sqrt{2\omega_{q\nu}}. \quad (1)$$

Here, N_k is the number of k points used in the summation, $N_{\sigma}(0)$ is the density of states per spin at the Fermi level, and $\omega_{q\nu}$ are the phonon frequencies. The e-ph matrix element $g_{kn,k+q,m}^{\nu,\sigma}$ is defined by the variation in the self-consistent crystal potential V_{σ} for the spin σ with respect to a frozen

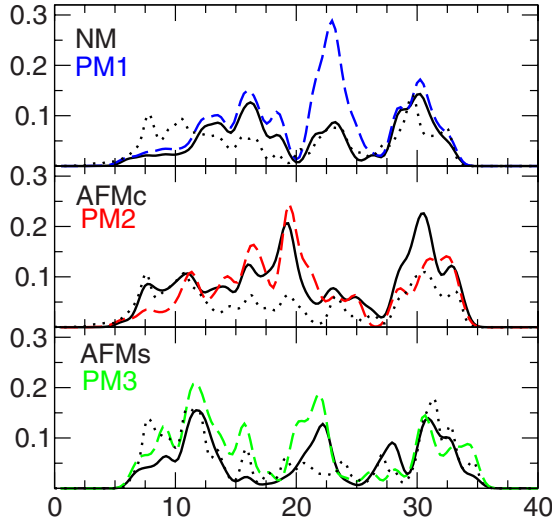


FIG. 2. (Color online) The Eliashberg functions $\alpha^2 F(\omega)$ for the NM (top, black solid line), AFM (middle and bottom, black solid lines), and model paramagnetic calculations, as described in the text, (PM1–3, colored dashed lines). The corresponding phonon densities of states, in arbitrary units, are shown in each panel by the dotted lines.

phonon displacement according to the phonon eigenvector $e_{q\nu} = \sum_{A\alpha} M_A \sqrt{2\omega_{q\nu}} \epsilon_{A\alpha}^{q\nu} u_{qA\alpha}$. Here $u_{qA\alpha}$ is the Fourier transform of the α component of the phonon displacement of the atom A in the unit cell, M_A is the mass of atom A , and $\epsilon_{A\alpha}^{q\nu}$ are $A\alpha$ components of $q\nu$ phonon eigenvector normalized in the unit cell. For an AFM system, $\alpha^2 F_{\uparrow\uparrow}(\omega) = \alpha^2 F_{\downarrow\downarrow}(\omega)$. In the following, we drop the spin indexes and consider: $\alpha^2 F(\omega) = \alpha^2 F_{\sigma\sigma}(\omega)$. The first inverse moment of $\alpha^2 F(\omega)$ gives the frequency-dependent e-ph coupling constant,

$$\lambda(\omega) = 2 \int_0^\omega d\Omega \alpha^2 F(\Omega) / \Omega. \quad (2)$$

The total e-ph coupling constant $\lambda = \lambda(\omega = \infty)$ is 0.18, 0.33, and 0.18 for NM, AFMc, and AFMs, respectively.

The three calculations in Fig. 1 have different phonon spectra $\omega_{q\nu}$, different self-consistent crystal potentials V_σ , and different one-electron wave functions $|\mathbf{k}n\rangle$ and eigenenergies $\epsilon_{\mathbf{k}}^\sigma$, which all determine the value of λ in Eqs. (1) and (2). In order to understand which of these factors dominates the e-ph coupling, we start for simplicity from the so-called Hopfield formula for the e-ph coupling constant,

$$\lambda = \frac{N_\sigma(0) D^2}{M\omega^2}, \quad (3)$$

where D is the deformation potential, which is a measure of the average e-ph interaction, and $M\omega^2$ is a characteristic force constant, which we assume depends weakly on the magnetic order. We can then use the ratio $\lambda/N_\sigma(0)$ to obtain an estimate for the average change in the e-ph interaction due to magnetism; going from NM to AFMc (AFMs), this ratio, and hence D^2 , increases by $\sim 50\%$, from 0.15 to 0.24 (0.26)—see Table I. A comparison of Eqs. (1) and (3) shows that the increase in D can be caused either by an increase in

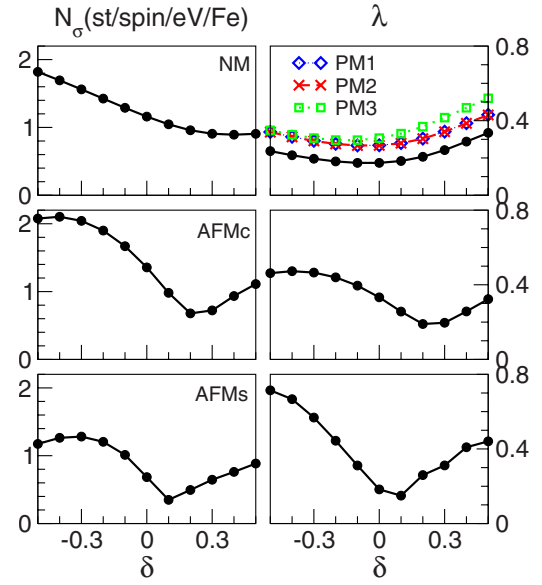


FIG. 3. (Color online) Effect of doping on the e-ph coupling of BaFe_2As_2 in the rigid-band model. $\pm\delta$ is the number of excess electrons/holes per Fe atom. The left panel shows the density of states at E_F , in states/spin eV Fe atom. The right panel shows the same-spin coupling constant $\lambda = \lambda_{\sigma\sigma}$. $N_\sigma(0)$ is the same for NM and all three (see text) PM calculations, as described in text.

the derivative of the DFT potential V_σ with respect to displacement, or by a difference in the one-electron wave functions, used to evaluate its average over the Fermi surface. In order to disentangle these two effects, we performed a mixed calculation (PM1), in which we combined the NM eigenvalues and wave functions, as well as the phonon frequencies, with the AFMc potential variations in the Eq. (1). In the top panel of Fig. 2, we compare the resulting Eliashberg function $\alpha^2 F(\omega)$ with the NM one; the total phonon DOS $F(\omega)$ is also shown as dotted lines. The effect of using the AFM potential is an increased coupling of electrons to phonons with frequencies $\omega \sim 20$ – 25 meV while other modes are largely unaffected. This increases λ from 0.18 (NM) to 0.27 (PM1). The middle and lower panel of Fig. 2 show two calculations, PM2 and PM3, which use NM one-electron wave functions, AFMc and AFMs phonon frequencies, and crystal potentials, respectively. A comparison of the $\alpha^2 F(\omega)$ with the phonon densities of states shows that, also in these cases, there is an increased coupling to phonons around 20 meV, both in AFM and PM. The λ 's, reported in Table I, are 0.27 and 0.31, for PM2 and PM3, respectively. From the comparison of PM1 and PM2, we conclude that the effect of the phonon frequency is negligible while the $\sim 10\%$ spread of values between PM2 and PM3 gives an indication of the effect of the short-range AFM correlations on λ . Finally, we find that the values of $\lambda/N_\sigma(0)$ in the PM calculations are in line with the AFM ones, indicating that, at $\delta=0$, the states at E_F have a comparable, weak coupling to phonons, for both NM and AFM orders.

These model calculations, which combine the AFM potentials and phonons and the NM wave functions and Fermi surfaces, represent the best approximation, at LDA level, of the real PM state of superconducting, doped, BaFe_2As_2

which is characterized by local, disordered magnetic moments.²² In the following, we will use them to estimate an upper bound for the e-ph coupling in the *doped* BaFe₂As₂.

In Fig. 3, we show the density of states at the Fermi level $N_{\sigma}(0)$ (left) and λ (right) as a function of doping δ for NM, AFMc, AFMs, and PM orders, from a rigid-band calculation; δ is defined as the number of excess electrons (holes) per Fe atom. NM and PM calculations have the same $N_{\sigma}(0)$, which decreases monotonically as a function of doping, while λ is roughly symmetric around $\delta=0$. This indicates that, in Eqs. (1)–(3), the effect of the matrix element dominates over that of the DOS. In the AFM calculations, the shape of the λ curve follows more closely than that of $N_{\sigma}(0)$, with a minimum at $\delta\sim 0.1$ – 0.2 , and a maximum $\lambda=0.8$ for AFMs at $\delta=-0.5$, corresponding to KFe₂As₂. However, the use of the rigid-band approximation is questionable at these high dopings, and in the following we limit our analysis to a smaller range of $\delta=\pm 0.25$, where the error in λ connected to the rigid-band approximation is $\lesssim 20\%$.²³

We can summarize the results of Fig. 3, by saying that, for $|\delta|<0.25$, an upper bound for the e-ph coupling in BaFe₂As₂ superconductors is $\lambda=0.35$. The enhancement in λ results from a $\sim 50\%$ increase in the e-ph matrix elements, due to local magnetism, which is independent on doping, and a

symmetric increase in the matrix element for $\delta\neq 0$, which does not follow the shape of the electronic DOS. The phonon softening in the magnetic calculations also enhances the e-ph coupling but the main effect is coming directly from the matrix elements. The value $\lambda=0.35$, which includes magnetism and doping, is almost a factor of two larger than that estimated in early nonmagnetic calculations for the undoped compounds,^{1,2} and close to a recent experimental estimate of λ from a kink in photoemission spectra.⁴

What are the consequences of this result? Of course, it cannot explain a T_c of 38 K, which confirms that superconductivity in this and other Fe-based superconductors is most likely due to electronic (magnetic) degrees of freedom.^{2,24} However, in Fe pnictides, studies of the superconducting gap in realistic models with AFM spin fluctuations show that solutions with and without gap nodes are almost degenerate, so that even a relatively low e-ph coupling constant can help select either of them, by enhancing/suppressing the pairing in the relevant channel.^{25,26}

L.B. wishes to thank O.K. Andersen for encouragement, support, and advice. Part of the calculations were performed at the IDRIS superconducting center.

¹L. Boeri, O. V. Dolgov, and A. A. Golubov, *Phys. Rev. Lett.* **101**, 026403 (2008); *Physica C* and **469**, 628 (2009).

²I. I. Mazin, D. J. Singh, M. D. Johannes, and M. H. Du, *Phys. Rev. Lett.* **101**, 057003 (2008).

³R. H. Liu *et al.*, *Nature (London)* **459**, 64 (2009); P. M. Shirage, K. Kihou, K. Miyazawa, C.-H. Lee, H. Kito, H. Eisaki, T. Yanagisawa, Y. Tanaka, and A. Iyo, *Phys. Rev. Lett.* **103**, 257003 (2009).

⁴A. Kordyuk, V. Zabolotnyy, D. Evtushinsky, T. Kim, I. Morozov, M. Kubic, R. Follath, G. Behr, B. Buechner, and S. Borisenko, [arXiv:1002.3149](https://arxiv.org/abs/1002.3149) (unpublished).

⁵M. Rahlenbeck, G. L. Sun, D. L. Sun, C. T. Lin, B. Keimer, and C. Ulrich, *Phys. Rev. B* **80**, 064509 (2009); K. Choi, P. Lemmens, I. Eremin, G. Zwicknag, H. Berger, G. Sun, D. Sun, and C. Lin, *J. Phys.: Condens. Matter* **22**, 115802 (2010).

⁶I. I. Mazin, M. D. Johannes, L. Boeri, K. Koepernik, and D. J. Singh, *Phys. Rev. B* **78**, 085104 (2008).

⁷T. Yildirim, *Phys. Rev. Lett.* **102**, 037003 (2009); *Physica C* and **469**, 425 (2009).

⁸M. Zbiri, H. Schober, M. R. Johnson, S. Rols, R. Mittal, Y. Su, M. Rotter, and D. Johrendt, *Phys. Rev. B* **79**, 064511 (2009); S. E. Hahn *et al.*, *ibid.* **79**, 220511(R) (2009).

⁹D. Reznik *et al.*, *Phys. Rev. B* **80**, 214534 (2009).

¹⁰I. I. Mazin and M. D. Johannes, *Nat. Phys.* **5**, 141 (2009).

¹¹M. D. Johannes and I. I. Mazin, *Phys. Rev. B* **79**, 220510 (2009).

¹²F. Yndurain and J. M. Soler, *Phys. Rev. B* **79**, 134506 (2009).

¹³T. Egami *et al.*, *Adv. Cond. Matter Phys.* **2010**, 164916 (2010); T. Egami, B. Fine, D. Singh, D. Parshall, C. de la Cruz, and P. Dai, [arXiv:0908.4361](https://arxiv.org/abs/0908.4361) (unpublished).

¹⁴S. Baroni *et al.*, *Rev. Mod. Phys.* **73**, 515 (2001).

¹⁵M. Rotter, M. Tegel, D. Johrendt, I. Schellenberg, W. Hermes, and R. Pöttgen, *Phys. Rev. B* **78**, 020503 (2008).

¹⁶The lattice constants, as well as the internal coordinate of the As atoms, are set to the experimental values: $a=3.96$ Å, $c=13.02$ Å, and $z_{\text{As}}=0.3545$.

¹⁷J. P. Perdew, K. Burke, and M. Ernzerhof, *Phys. Rev. Lett.* **78**, 1396 (1997).

¹⁸P. Giannozzi *et al.* (unpublished), <http://www.quantum-espresso.org>

¹⁹D. Vanderbilt, *Phys. Rev. B* **41**, 7892 (1990).

²⁰D. J. Singh, *Phys. Rev. B* **78**, 094511 (2008).

²¹Notice that the magnetic moment reported in Table I is actually the integral of the absolute value of the magnetization over the cell, and therefore larger than the moment inside the Fe muffin-tin sphere, usually quoted in linearly augmented plane waves (LAPW) calculations.

²²P. Hansmann, R. Arita, A. Toschi, S. Sakai, G. Sangiovanni, and K. Held, *Phys. Rev. Lett.* **104**, 197002 (2010).

²³The accuracy of the rigid-band approximation is difficult to access quantitatively, given that the e-ph coupling is sensitive not only to the band structure, but also to the magnetic moments and the deformation potential. However, we have verified that for the doping $|\delta|=25\%$ the DOS of the entire Fe-derived band, calculated in the corresponding supercells, and in the virtual crystal approximation, remains rather close (i.e., $\pm 10\%$) to the rigid-band DOS, therefore we consider application of the rigid-band approximation in this interval to be meaningful.

²⁴K. Kuroki, S. Onari, R. Arita, H. Usui, Y. Tanaka, H. Kontani, and H. Aoki, *Phys. Rev. Lett.* **101**, 087004 (2008).

²⁵I. I. Mazin and J. Schmalian, *Physica C* **469**, 614 (2009).

²⁶K. Kuroki, H. Usui, S. Onari, R. Arita, and H. Aoki, *Phys. Rev. B* **79**, 224511 (2009); A. Kemper, T. Maier, S. Graser, H. Cheng, P. Hirschfeld, and D. Scalapino, [arXiv:1003.2777](https://arxiv.org/abs/1003.2777), *New J. Phys.* (to be published); R. Thomale, C. Platt, W. Hanke, and B. Andrei Bernevig, [arXiv:1002.3599](https://arxiv.org/abs/1002.3599) (unpublished).